

Overview on Calorimetry

Erika Garutti^a

^a*Deutsches Elektronen-Synchrotron (DESY), Hamburg, Germany*

Abstract

In this paper I want to review the state of the art of calorimeter developments. I will focus on innovative solutions in calorimetry at the technology frontier and I will favor calorimeters for High Energy Physics detectors. The field in which calorimeters find their application is so broad that this short review does not do justice to all ongoing projects. Instead, this paper shall be considered as a collection of currently hot topics on the subject.

Key words: calorimeter, particle flow, dual readout, silicon photomultiplier.

1. Introduction

The focus of this review is on the frontier of calorimeter technology. The largest and most complex calorimeters are probably still those developed for HEP detectors at collider machines. The physics challenge for the next generation of HEP detectors will be to improve the jet energy resolution by about a factor of two with respect to existing calorimeter systems. Jet reconstruction is the driving theme of ongoing R&D activities in the HEP field.

The calorimeter for high performance jet physics has to be designed to fit inside a realistically large magnetic coil. Therefore, a homogeneous calorimeter, especially for the hadronic part, is excluded. The current technology choice is that of sampling structures alternating dense passive materials - like copper, steel or tungsten - and active readout materials - like plastic scintillators, silicon or gaseous chambers. Two major approaches are being considered which have the potential to significantly improve the jet energy resolution at future experiments. One approach is based on the idea of reducing fluctuations in the hadronic shower reconstruction, which are the main responsible of the jet energy deterioration. As homogeneous calorimeters are not a viable solution inside the magnetic coil, an alternative to compensation is to measure independently the electromagnetic and the neutral component of a hadronic shower and to correct event-by-event for the different response of the calorimeter to various particle types. This is the method known as dual/triple readout [1], and more details on this technique and on the first R&D results will be given in section 2.

An alternative approach is the so-called particle flow, namely the reconstruction of the four-momentum of every single particle of every event recorded in a detector. This method requires a detector with unprecedented granularity in both longitudinal and lateral segmentation, combined with a sophisticated reconstruction algorithm capable of single particle separation. Latest results on particle flow studies are reported in [2]. More details on the proposed calorimeters for particle flow are given in section 3.

Section 4 is a brief overview of some recent technological developments driven by calorimetry requirements.

2. Dual/Triple readout calorimetry

The energy resolution of calorimeters is determined by fluctuations. In order to improve this resolution significantly, the dominating sources of these fluctuations have to be addressed. In almost all calorimeters, i.e. the ones with $e/h \neq 1.0$, fluctuations in the electromagnetic shower fraction (f_{em}) dominate the energy resolution for hadrons and jets. These fluctuations, and their energy-dependent characteristics, are also responsible for other undesirable calorimeter characteristics, in particular hadronic signal non-linearity and a non-Gaussian response function. There are two possible approaches to eliminate (the effects of) these fluctuations: by designing the calorimeter such that the response to electromagnetic and non-electromagnetic energy deposit is the same (compensation, $e/h=1.0$), or by measuring f_{em} event-by-event. The DREAM collaboration [3] follows the latter approach and designs a Dual REAdout Module (hence the name DREAM).

Calorimeters based on Cerenkov light as the signal source are, for all practical purposes, only responding to the electromagnetic fraction of hadronic showers [4]. This is because the electrons/positrons through which the energy is deposited in the electromagnetic shower component are relativistic particles down to energies of only 200 keV. On the other hand, most of the non-electromagnetic energy in hadron showers is deposited by non-relativistic protons generated in nuclear reactions [4]. However, in other types of active media (scintillator, LAr) such protons do generate signals. The DREAM detector uses two active media: scintillating fibers measure dE/dx , while clear fibers measure the Cerenkov light generated in the shower development. By comparing the two signals, f_{em} can be measured event-by-event, and the total shower energy can be reconstructed using the known e/h value(s) of the calorimeter. The DREAM calorimeter, as well as many results obtained

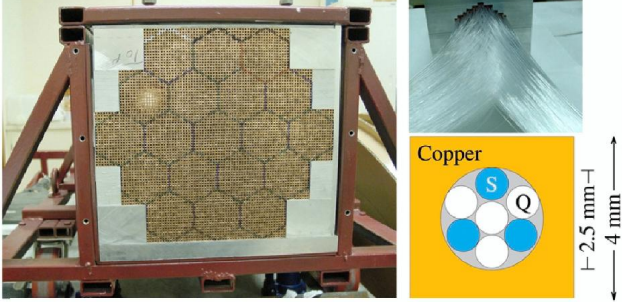


Figure 1: The DREAM calorimeter module viewed from the front (left), and a view of the fiber separation in the rear of one hexagonal cell (top, right). Cerenkov and scintillator fibers in each cell are read out by two separate PMTs. Each cell consists of several copper tubes containing each 4 clear Quartz fibers and 3 scintillating fibers (bottom, right).

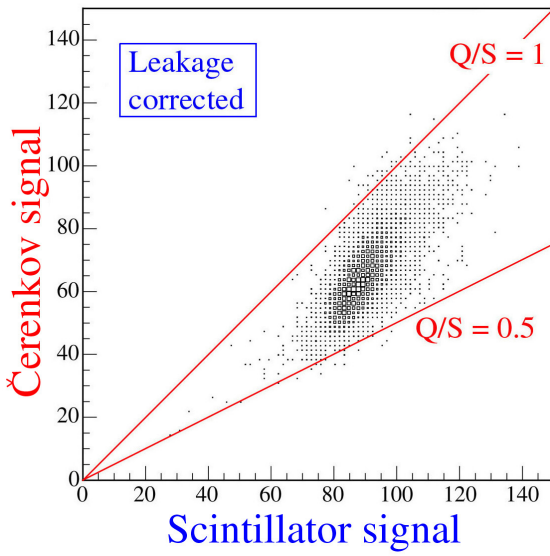


Figure 2: Correlation of the signal from Quartz fibers (Cerenkov signal) and scintillator fibers in the DREAM calorimeter, for a 100 GeV pion shower.

in beam tests of this device, have been described in detail in a number of papers [5, 6].

The basic element of the detector (Fig. 1) is a hollow, extruded copper tube, 200 cm long and 4×4 mm² in cross section. Seven optical fibers are inserted in the 2.5 mm wide hole, 3 scintillating fibers and 4 clear Quartz fibers for detecting Cerenkov light. The detector consists of about 6000 such tubes and contains in total 90 km of fibers. The fibers as they exit at the rear are split into bunches of the two different types of fibers. In this way, a hexagonal readout structure is created. Each hexagonal cell is read out by two PMTs, one for each type of light. Using the ratio of the two signals, the value of f_{em} in each hadronic shower is determined event-by-event in a straightforward way. Two values (0.5 and 1) for the ratio Q/S of Cerenkov (from Quartz fibers) to scintillation signal are represented by straight lines in the scatter plot of the two signals (Fig. 2).

Using the value of f_{em} , the signals are corrected for the effects of non-compensation. By this procedure the energy resolution improves, the signal distribution becomes more Gaussian and,

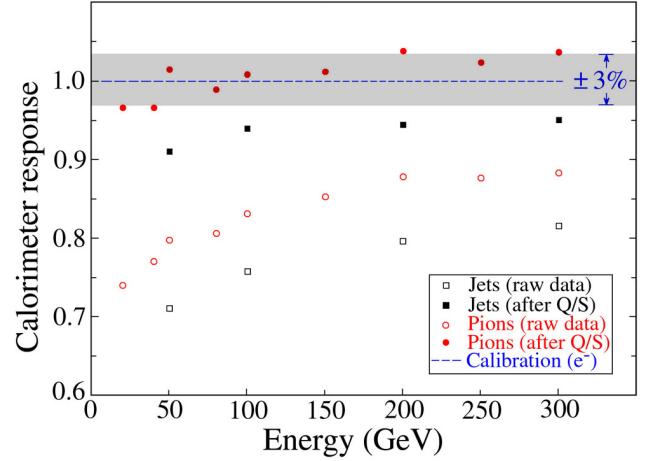


Figure 3: The DREAM response to single pions and high-multiplicity jets, before and after corrections made on the basis of the measured Cerenkov/scintillator signal ratio (Q/S).

most importantly, the hadronic energy is correctly reproduced. Fig. 3 shows the effect of the Q/S correction on the linearity of the calorimeter response. The strong non-linear behavior present in the raw data (open symbols) is corrected to better than 3% for single pions after applying this compensation technique (closed symbols).

The improvement in the energy resolution is visible in Fig. 4. For single pion showers the non-compensating response from the scintillator fibers gives a resolution with a stochastic term of $49\%/\sqrt{E}$. After correction using the Q/S ratio the stochastic term is improved to $41\%/\sqrt{E}$.

The benefit of the dual readout in reducing the intrinsic fluctuations in a hadronic shower is evident from the improvement of the energy resolution. The next step in dual readout calorimetry is the implementation of a third fiber material or, most promising, the time readout of the scintillation fibers

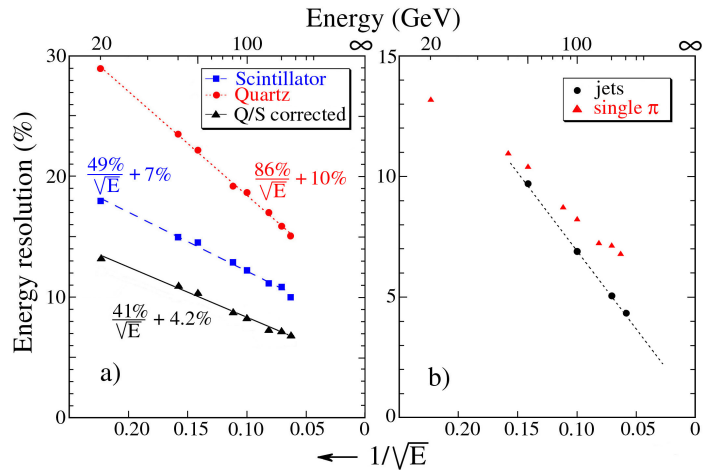


Figure 4: The energy resolution for single pions as a function of energy, measured with the scintillation fibers and the Cerenkov (Quartz) fibers, and after corrections made on the basis of the measured Q/S signal ratio. For the abscissa, the energy E is given in GeV (top scale) and in terms of $1/\sqrt{E}$ (bottom scale).

to measure the (slow) MeV neutrons produced in a hadronic shower, thereby suppressing the binding energy loss fluctuations. This latter method is referred to as triple readout and is being further tested by the DREAM collaboration.

One issue still to be addressed in the DREAM design presented above is the total absence of longitudinal segmentation. In order to recover at least the separation between the electromagnetic and the hadronic part of the calorimetric system, an alternative design of a hybrid dual readout calorimeter has been proposed. The electromagnetic section (ECAL) of this instrument consists of crystals (BGO or similar) and the hadronic section is the DREAM fiber prototype. The main goal is to demonstrate that a dual readout is also possible from the crystals, separating the (fast, directional) Cerenkov and scintillator response in order to obtain the Q/S ratio needed for compensation corrections. Realization and results of this prototype are discussed in detail in [7].

3. Particle flow calorimetry

In recent years the concept of high granularity particle flow calorimetry [8] has been developed in the context of the proposed International Linear Collider (ILC). The CALICE collaboration [9] is the major developer of calorimeter concepts and technologies for highly granular detectors for particle flow. All proposed calorimeter designs are sampling structures using tungsten as absorber material for the electromagnetic, and steel or tungsten for the hadronic calorimeters.

Here, a brief overview of the technologies chosen for the active layers is given, together with a description of the major R&D efforts and results.

3.1. High granularity with plastic scintillator readout

In order to use plastic scintillators for a highly granular readout, small scintillator tiles or strips are cast or extruded, with a typical size of 1-5 cm² for electromagnetic applications and ~10 cm² for hadronic applications. The typical thickness of the active layer is 0.3-0.5 cm, what allows a longitudinal segmentation of each calorimeter component into 30 to 40 layers. Each single calorimeter cell is read out via a silicon-based photo-detector (SiPM) mounted directly on the tile. The scintillation light can be collected via a wavelength shifting fiber inserted into the scintillator material and is then transported to the face of the photo-detector, as shown in Fig. 5.

With this technique calorimeter layers have been built, like the active layer of the analog hadronic calorimeter (AHCAL, [10]) depicted in Fig. 6.

The new generation of SiPMs offers more sensitivity in the blue spectral region, as opposed to the first devices which had a good green sensitivity quickly dropping in the blue range. With this photo-detectors it is possible to consider calorimeter cells without wavelength shifting fibers. If the scintillation light is directly coupled to the SiPM mounted on the tile, one has to worry about the homogeneity of the tile response. A detailed study of the tile response for various coupling combinations of SiPM and scintillator is given in [11].

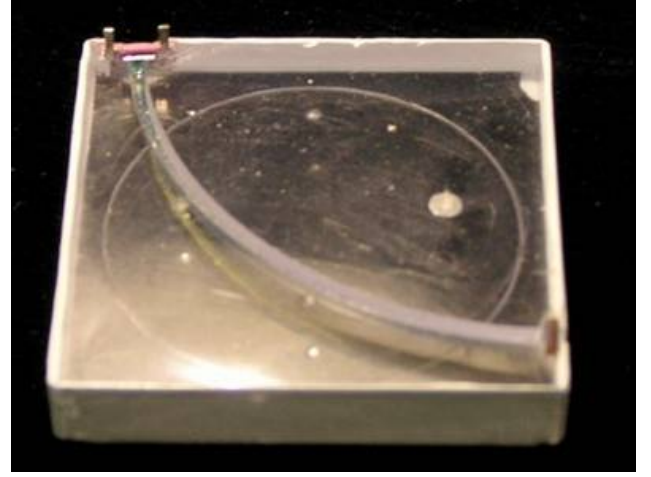


Figure 5: Scintillator tile with wavelength shifting fiber and SiPM readout. The picture shows a single calorimeter cell of the AHCAL prototype from CALICE.

CALICE has developed two prototypes based on scintillator/SiPM technology: an electromagnetic calorimeter with strips of 1×4.5×0.3 mm³ [12], and the hadronic calorimeter shown in Fig. 6. Both prototypes have been extensively tested at test beam facilities at DESY, CERN and FNAL.

A striking result deriving from high granularity is the significant improvement of the energy resolution obtained when applying energy density weighting techniques to achieve software compensation in hadronic showers. The fractions of the electromagnetic and of the hadronic component in a hadronic shower largely fluctuate event-by-event. Fig. 7 shows the strong correlation between the energy deposited in cells with a large energy density (cells measuring a large electromagnetic fraction) and the total energy deposited in the calorimeter by a 20 GeV pion shower. Events with a large electromagnetic fraction lead to larger reconstructed energies than those with a large hadronic fraction. This correlation was used to apply a weighting correction which improved the stochastic term of the energy resolution from 61%/√E to 49%/√E (see [13, 14] for more details).

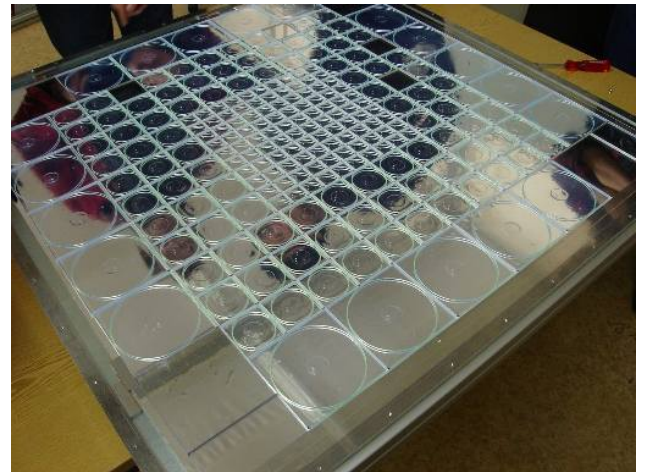


Figure 6: One active layer of the AHCAL prototype from CALICE.

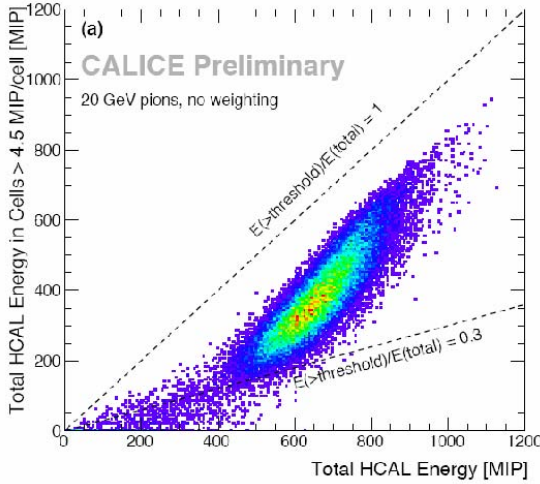


Figure 7: Correlation between the electromagnetic fraction (high energy density cells) and the total energy of a 20 GeV pion shower reconstructed in the AHCAL.

3.2. High granularity with gaseous detectors

An alternative way to further increase the granularity of a hadronic calorimeter, from $O(10 \text{ cm}^2)$ to $O(1 \text{ cm}^2)$, is to read out the individual cells in a digital way, i.e. neglecting the amplitude of the energy deposited in the cell. Simple Monte Carlo simulations indicate that this method could work for cells of 1 cm^2 size. Fig. 8 shows the linear correlation between the number of cells fired by a neutral hadron shower and the corresponding reconstructed energy.

Based on this principle prototypes of digital hadronic calorimeters are being developed, which use gas chambers with pad readout as active media. The amplification of the ionization signal in the gas is obtained either using resistive plate chambers (RPC, [15, 16, 17]), or Gas Electron-Multiplier foils (GEM, [18, 19]), or MICROMEAS layers [20, 21]. The realization of a large gas chamber as active layer of a calorimeter

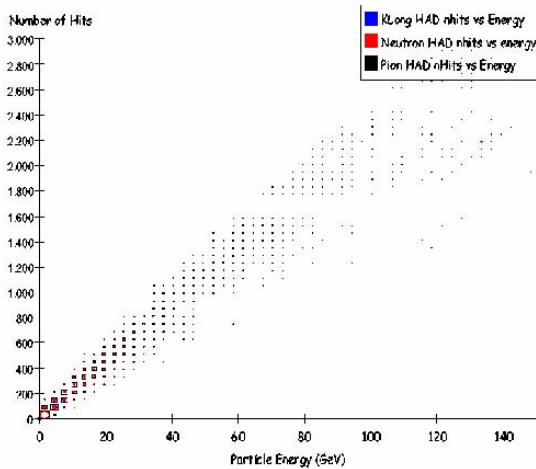


Figure 8: Monte Carlo simulation showing the linear correlation between the number of cells fired by a neutral hadron shower in a calorimeter with 1 cm^2 cell size and the corresponding reconstructed energy.



Figure 9: One step in the assembly of an active layer for a digital hadronic calorimeter using resistive plate chambers. The spacers separating the two glass plates are visible as lines inside of the area surrounded by the gas tight frame. The chamber has a size of about $32 \times 96 \text{ cm}^2$ and the distance between the two glass plates is 1.1 mm.



Figure 10: Front-end board integrated in one of the active layers of the digital hadronic calorimeter with RPC.

poses several challenges. The first being the mechanical stability of a gas volume of typically $30 \times 100 \text{ cm}^2$ enclosed by two glass plates, each 1.1 mm thick and separated by a gap of 1.1 mm. Fig. 9 shows one step in the assembly of such an active layer: the spacers separating the two glass plates are visible as lines inside of the area surrounded by the gas tight frame. The chambers are read out by $1 \times 1 \text{ cm}^2$ pads and the front-end electronics is located directly above. The thickness of each layer is less than 9 mm.

The front-end board carries the chips to read out up to 1526 pads, and it is placed on top of a given chamber. Fig. 10 shows one such PCB board equipped with 48 DCAL chips [22].

The digital HCAL technology has been already tested with a small size prototype [23] of $20 \times 20 \text{ cm}^2$ lateral size and 9 layers in depth, alternating RPC gas chambers and 2 cm thick steel plates. This prototype was exposed to a beam at the FNAL test beam facility. Fig. 11 displays an event with an 8 GeV/c pion undergoing an interaction between the 1st and the 2nd layer of the calorimeter.

Alternative technologies of gas amplification with GEM and MICROMEAS are also being pursued by the CALICE collaboration. The current status of the various R&D efforts is reported in [24].

3.3. High granularity with silicon readout

The main technology chosen for the readout of a highly granular electromagnetic calorimeter is based on high resistivity

$6 \times 6 \text{ cm}^2$ silicon wafers divided in $1 \times 1 \text{ cm}^2$ pad diodes. A sampling detector was assembled alternating $524 \mu\text{m}$ thick silicon layers with tungsten layers of a thickness increasing from 1.4 to 4.2 mm. Details of this design and of the results obtained with the first Si-W ECAL prototype are discussed in [25] and [26].

As in the hadronic calorimeter case, also for the electromagnetic calorimeter an alternative technology exists to read out the data in a digital way. In order to count charged particles with binary readout, the pixel size must be much smaller than the separation of particles within the showers so that the probability of two particles hitting the same pixel is kept small. A naive study with $1 \times 1 \text{ cm}^2$ cells, as presented in Fig. 12, illustrates the problem of a non-linear correlation between the deposited energy and the number of fired cells if the granularity is not sufficient. According to simulations, the density of charged particles in the innermost core of the highest energy electromagnetic showers expected at the ILC may have a tail reaching up to around 100 mm^{-2} . However, high energy electromagnetic showers have not been measured accurately at a high level of granularity. The knowledge of the actual shower density is clearly critical for the optimization of the pixel size, and this is one of the major initial aims of the first prototype of a digital ECAL (DECAL). For the studies performed so far, a pixel size of $50 \times 50 \mu\text{m}^2$ has been assumed. This would require an ECAL for an ILC detector to have around 10^{12} pixels.

One basic motivation for a DECAL is that there is potentially a significant improvement in the electromagnetic shower resolution. Fig. 13 allows a comparison of the imaging capability between a calorimeter with such an extreme granularity and a conventional highly granular analog ECAL with 16 mm^2 cells size.

ECALs usually work on the principle that the number of charged particles passing through each layer is on average proportional to the incident particle energy; there are fluctuations around this average due to the stochastic nature of the shower development. These charged particles lose energy in traversing the sensitive layers of the ECAL, and the energy loss per particle also has fluctuations, mainly due to the Landau distri-

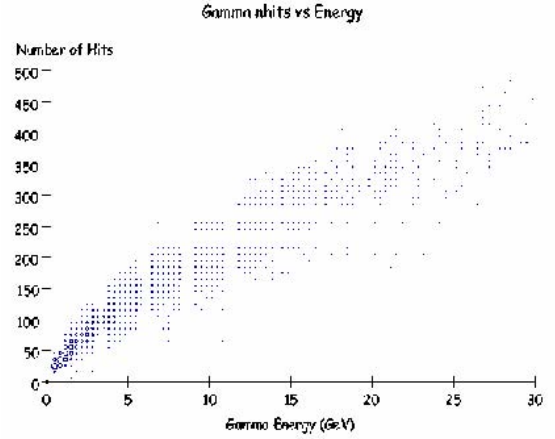


Figure 12: Monte Carlo simulation showing the non-linear correlation between the number of cells fired by a photon shower in a calorimeter with 1 cm^2 cell size and the corresponding reconstructed energy.

bution of the deposited energy but also due to variations in their speed and path length through the material. An analog ECAL therefore has contributions to the energy resolution both from the intrinsic shower fluctuations and also from the variations of the energy per charged particle. The basic idea of a DECAL would be to reduce (or eliminate) the latter contribution by attempting to measure the number of charged particles directly. Fig. 14 shows an example of the fundamental resolution for electromagnetic showers simulated in an analog and in a digital calorimeter of the same geometry. In both cases the plotted resolutions are “ideal”, meaning they are based on perfect information with no dead regions, electronics noise, threshold suppression etc. It is thought that a realistic analog ECAL will approach this idealized value, and the purpose of the DECAL studies is to determine the degree to which this is true for the digital case. Simulation studies so far indicate a degradation in the stochastic term from $12.8\%/\sqrt{E}$ to around $14.0\%/\sqrt{E}$; this is still better than the ideal analog case. A major uncertainty

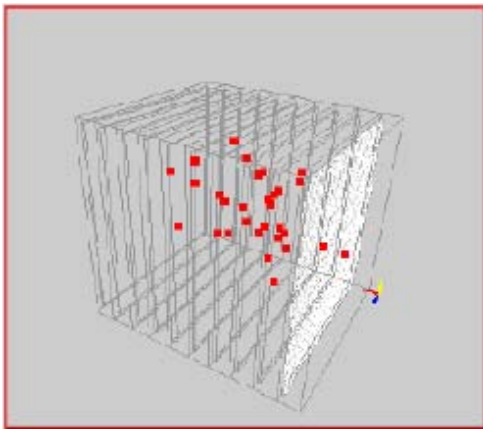


Figure 11: Event display of a pion induced shower with an interaction between the 1st and the 2nd layer (counting from the right) in the digital hadronic calorimeter prototype described in [15].

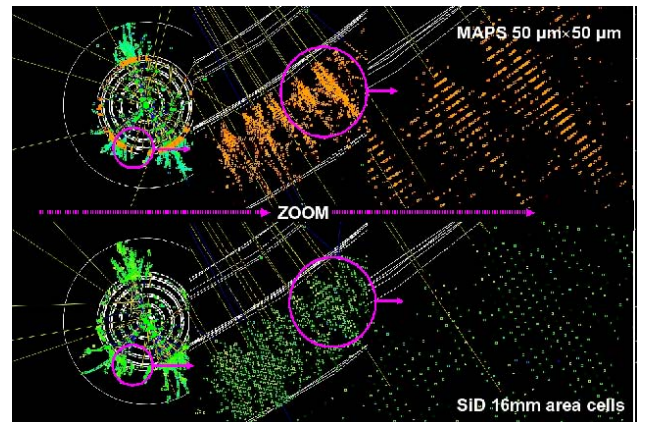


Figure 13: Comparison of the imaging capability between a digital ECAL with extreme granularity ($50 \times 50 \mu\text{m}^2$ cell size) and a conventional highly granular analog ECAL with 16 mm^2 cells size. The same hadronic jet is simulated for the two detector options.

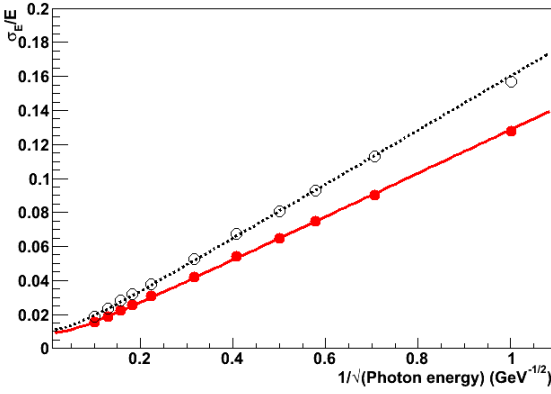


Figure 14: Simulated resolution of electromagnetic showers in ideal analog (open circles) and digital (filled circles) ECALs with the same geometry. The lines show the results of fits to the data points in the form $\sigma_E/E = a \oplus b/\sqrt{E}$ in GeV, yielding $a = 0.9$, $b = 0.128$ for the digital case and $a = 1.1$, $b = 0.160$ for the analog case.

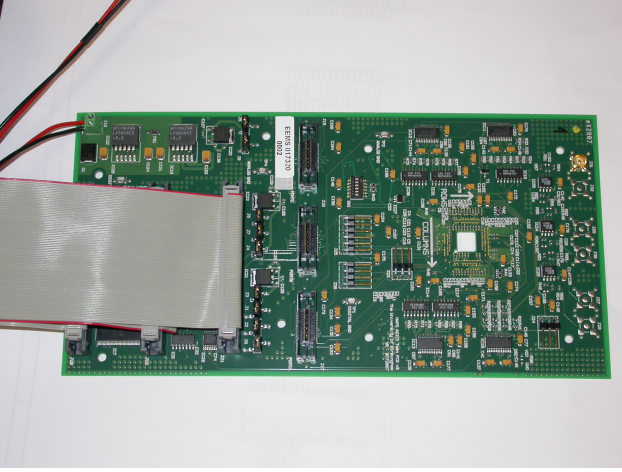


Figure 15: One layer of the digital ECAL prototype stack, showing the TPAC sensor mounted on the PCB as the small silver square.

in this more realistic resolution is the core shower density, as mentioned above; hence the need to measure this directly.

A viable technical solution for a digital ECAL is to use Monolithic Active Pixel Sensors (MAPS), a standard CMOS product developed originally for vertex detectors. The SPIDER collaboration [27] has tested a stack of six layers each equipped with one TPAC sensor based on MAPS technology. One digital ECAL layer is shown in Fig. 15. A small silver square is visible on the picture corresponding to the TPAC sensor. Each sensor has an active area of $8.4 \times 8.4 \text{ mm}^2$ and a total of ~ 28000 pixels. This test and the successful data taking with these sensors in a beam represent the first steps to establish the MAPS technology as a possible solution for calorimetric applications. More details on this technology and on the test beam results can be found in [28].

3.4. From the proof-of-principle to scalable detectors

The development of calorimeter prototypes generally proceeds in two steps. Physics prototypes provide a proof-of-

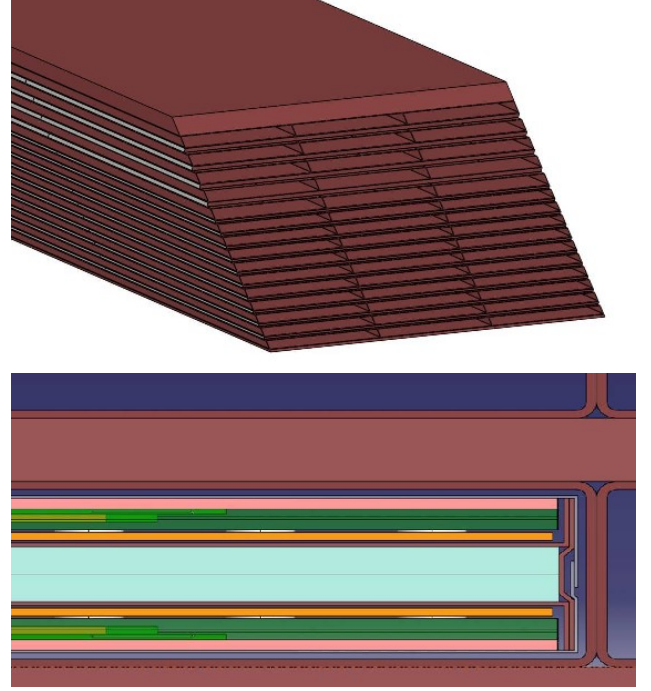


Figure 16: Design of the Si-W ECAL technical prototype.

principle for the viability of a given technology in terms of construction, operation and performance. In addition, they are used to collect large data sets for the study of the hadronic and electromagnetic shower evolution with high granularity, for the test of shower simulation programs, and for the development of particle flow reconstruction algorithms with real data. Technological prototypes address the issues of scalability, integration and cost optimization. The prototypes discussed so far are all of the first kind. A technological prototype is more a second generation development of the first R&D version, it is tailored to a specific application in a given experiment, and it tries to address as many integration and scalability issues as possible. Each proposed technology for the next generation detectors, for instance at the International Linear Collider, is now being taken to this next level of sophistication.

To give an example, the technical prototype of the Si-W ECAL is conceived as a slightly smaller scale version of a single module of the final ECAL detector. It has the same shape as the ILD [29] ECAL module design, the same number of layers, but somewhat smaller transverse dimensions (see Fig. 16).

This next generation of silicon detectors will have a granularity four times higher than in the physics prototype, with a cell size of $5 \times 5 \text{ mm}^2$. To minimize the effect of dead areas at the edges of the silicon sensors, larger $9 \times 9 \text{ cm}^2$ sensors have been developed.

In contrast to the physics prototype, where the front end electronics was placed outside the detector volume, the technical prototype will have the electronics directly embedded in the PCBs which support the silicon detectors. This requires the design of ambitiously thin and complex PCBs, and dedicated studies for the bonding and the encapsulation of unpackaged

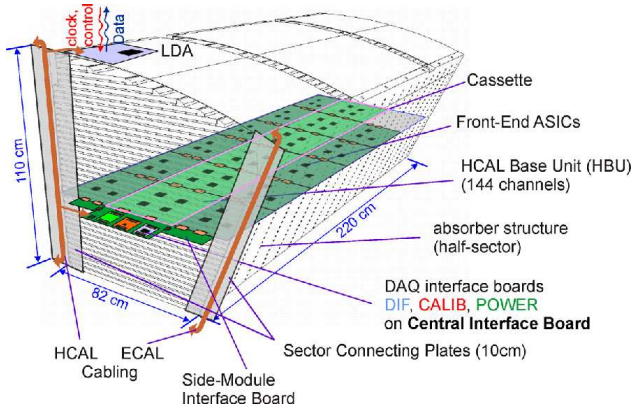


Figure 17: Electronics integration architecture for the technological AHCAL prototype.

chips. The space available for the PCB is limited and, to avoid degrading the detector performance, it must have a height of not more than 1.2 mm.

The front end chips must consume very little power to prevent massive cooling requirements. They should in particular make use of the ILC bunch structure, where beam is delivered to the detectors only in about 1% of the time. A power-pulsed design of the electronics will allow the chips to be powered for only the time when beam is delivered (plus some readout time). Thus the chips will be powered down for the remaining $\sim 99\%$ of the time. The zero-suppressed, digitized signals from the front-end electronics will then be passed to the common CALICE DAQ system.

In analogy to the ECAL case, the analog HCAL technology as well is moving in the direction of a scalable detector concept. In order to validate the concept of a highly granular scintillator-based HCAL, it needs to be demonstrated that the high channel density can actually be realized without compromising the performance by too many dead spaces or by the reduced compactness and hermeticity once readout and calibration electronics or the support structures have been accommodated. In this respect, the physics prototype is not scalable and needs to be complemented by technological prototypes addressing these integration issues.

The envisaged detector architecture is sketched in Fig. 17. It is inspired by the ILD¹ variant of a detector for the ILC, but it is very similar to the SiD² variant or to a detector for the Compact Linear Collider (CLIC³). The figure shows one sector of a barrel subdivided only once along the beam axis. This layout provides access to electronics and service interfaces once the detector end-cap is opened, but it poses tight space constraints on the transition region between barrel and end-cap.

There are 48 independent read-out layers which must be as thin as possible in order to keep the overall detector volume small, as it has to fit inside the main solenoid of the collider detector and still provide maximum hadronic absorption depth.

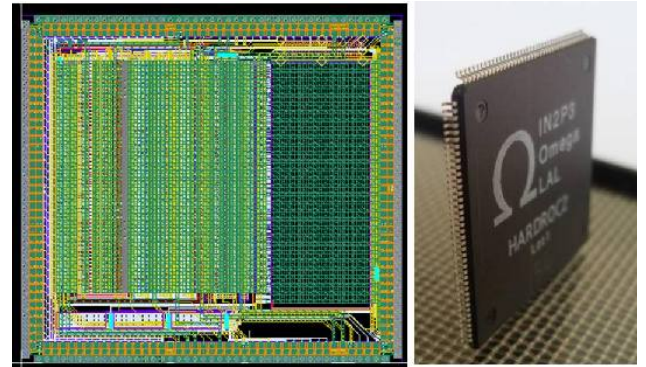


Figure 18: Layout of the SPIROC chip for readout of 36 SiPMs (left). Packaging of the HARDROC2 chip for the readout of the digital HCAL (right).

Each layer has a fine transverse segmentation, again with individual cell read-out, what requires concentrating the data at an early stage in order to keep connectivity issues manageable and to reduce dead areas occupied by external electronics components.

The SPIROC ASIC, which reads 36 SiPMs, includes the analog and digital treatment of the signals. It has an analog memory to record up to 16 events of a train and auto-triggering capability. The first prototype was fabricated in June 2007 in AMS SiGe $0.35\mu\text{m}$ technology [30]. The chip layout is shown in Fig. 18. Its area is 35 mm^2 for 36 channels. Due to the operation with pulsed power synchronous with the accelerator time structure, no cooling inside the modules is necessary. The total power consumption for the whole chip during the “power off” state is reduced to a few μW , and an average of $25\mu\text{W}$ per channel is expected during operation.

It is expected that, over the next years, prototypes of each technological option will become available and will be taken to test beams in an extensive campaign to pave the way for the construction of an ILC detector.

4. New developments at the technology frontier

Driven by calorimetric applications, many technologies are being improved and pushed to always better quality. It is worth to report on two very interesting developments that find their main application in calorimeters: Silicon-Photomultipliers and inorganic crystal fibers.

4.1. Silicon-Photomultipliers

The research on Silicon-Photomultipliers was a booming field over the last ten years. The application of SiPMs has been considered by most of the HEP experiments involving light detection techniques. I find it relevant for this review to give a list of the currently known SiPMs and their main differences. It is beyond the scope of this paper to review the principle of operation, and the full set of parameters that can be optimized when working with these devices. For this purpose, I refer the reader to specific publications like [31, 32, 33] or [34, 35, 36].

¹<http://www.ilcild.org/>

²<https://confluence.slac.stanford.edu/display/SiD/>

³<http://cllc-study.web.cern.ch/>

Probably the best known and widely-used SiPM is the Multi-Pixel Photon Counter (MPPC) from Hamamatsu⁴. This is a reliable, mass produced device, which was the first to offer enhanced sensitivity in the blue spectral region. The exact quantification of the photon detection efficiency (PDE) of this device has opened a long discussion in the community; a well documented measurement of the PDE can be found in [37]. The MPPC comes in various formats with a single-pixel size of 25-100 μm , with the PDE increasing as the pixel size increases. In general, these detectors have a very good performance in terms of all key parameters, as dark-rate (<MHz at 0.5 p.e. threshold), inter-pixel cross talk ($O(10-15\%)$), and gain ($3-8 \times 10^5$). With respect to this product, there exist several other devices which were developed to offer better performance relative to one or the other parameter.

If a large dynamic range is required for a specific application, the MAPD from Zecotek⁵ may be the solution, each device offering in the order of 15000 pixels/mm². MAPDs are also known to have low dark rate and inter-pixel cross talk. Possibly they are also radiation harder [38] than other SiPMs, though at the price of a lower gain of $O(3-5 \times 10^4)$.

For a reliable mass production of a large amount of sensors the SensL⁶ SiPM is a good choice. This device does not offer very aggressive parameters but they remain stable over a large-scale production.

A product with longer recovery time than the MPPC is the CPTA⁷ SiPM. A longer recovery time leads to a smaller after-pulse and cross-talk, so in general a smaller noise above threshold, when the threshold is set above the first photo-electron peak.

For some applications more UV-sensitive devices are desirable: here the company KETEK⁸ has presented an interesting prototype of a SiPM worth being investigated.

A new development, in the direction of a simplified design for SiPMs and aiming at improved quality, is the SiMPL from MPI Munich [39]. This innovative device is based on a different solution for the quenching resistor integrated into the silicon bulk, which does not require the typical poly-silicon resistor on the surface of SiPMs. By this approach, the geometrical fill factor is significantly improved and, as a consequence, the PDE is increased. Due to the very simple production process and because of the relaxed lithography requirements, a significant cost reduction in the mass production of the SiMPL is expected.

Many more SiPM devices, supplied by many SiPM producers, are currently available on the market, but they could not be covered in this review. Hence the community can expect significant improvements still to come.

4.2. Inorganic crystal fibers

Continuous innovations in the field of materials are following the increasing demands on calorimeters. Inorganic crystal ma-



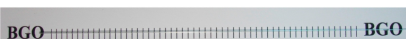
LYSO:Ce	
YAG:Ce	
BGO	

Figure 19: Examples of various crystal fibers produced by Fibercryst.

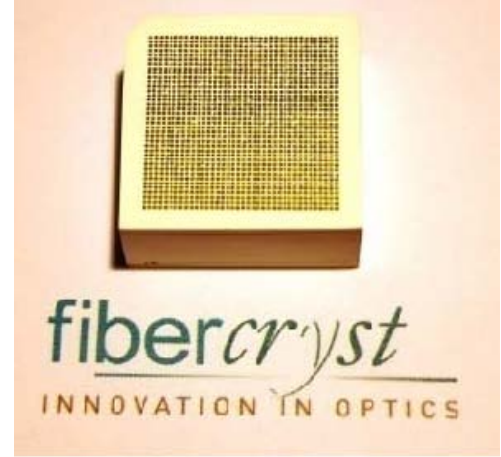


Figure 20: Demonstrator array of LuAg:Ce fibers of 400 μm diameter, produced by Fibercryst.

terials and crystal growing techniques are examples of the incredible impact calorimeters have on technology developments.

Following the idea of dual/triple readout calorimetry, it is natural to envisage bundles of fibers of two or three different materials measuring light produced by dE/dx or by the Cerenkov effect, or of material more sensitive to neutrons (i.e. hydrogenous materials). Such bundles would provide the active media of a calorimeter. If these fibers can be made of very dense material, like inorganic crystals, they could constitute the entire calorimeter material, without requiring a dense absorber and with all the advantages of a homogeneous calorimeter [40]. These and other ideas have pushed the development of crystal fibers. A novel production method has been established: the Micro-Pulling-Down crystal growth technique by companies like Fibercryst⁹, which allows the growth of scintillating fibers with composition such as Ce, LuAG, Ce:YAG, Ce:LYSO, BGO (Fig. 19). These fibers exhibit scintillation properties comparable to the scintillator crystals grown by the conventional Czochralski method.

Fibers with a total length of several tens of meters were produced for testing. An array, a prototype for imaging, has been assembled with 400 μm LuAG:Ce fibers (Fig. 20). Presently, fibers made of compositions such as LuAG or YAG doped with trivalent cerium have been developed and have reached an industrial level. Circular shapes are available with a diameter ranging from 350 μm up to 3 mm, but other shapes (square, hexagonal) are also possible.

⁴<http://www.hamamatsu.com/>

⁵<http://www.zecotek.com/>

⁶<http://sensl.com/products/>

⁷<http://www.cpta-apd.ru/>

⁸<http://www.ketek.net/>

⁹<http://www.fibercryst.com/>

5. Conclusions

Calorimetry is an active and vital field in continuous development. Calorimetry at the technology frontier drives the development of new materials, of new photo-detectors, of new electronics and of more general, new ideas and techniques to achieve the best possible detector for every specific application.

The present key questions of HEP calorimeters are focused on extreme segmentation (small cells) in the direction of imaging calorimetry; on extreme integration to maximize the hermeticity of the detectors; and on various solutions to achieve compensation in a limited volume (inside a realistic magnetic coil). The two approaches of dual/triple readout and of particle flow have been discussed as two alternatives to address this latter problem.

6. Acknowledgments

I want to thank the organizers of the VCI2010 conference for giving me the opportunity to present this review. Many thanks to the colleagues who have allowed me to use their material and work, in particular: the entire CALICE collaboration; Gabriella Gaudio, John Hauptman, Richard Wigmans from the DREAM collaboration; Paul Dauncey and Nigel Watson from the SPIDER collaboration.

References

- [1] N. Akchurin *et al.*, “Hadron And Jet Detection With A Dual-Readout Calorimeter,” Nucl. Instr. and Meth. A 537 (2005) 537.
- [2] M. A. Thomson, “Particle Flow Calorimetry and the PandoraPFA Algorithm,” Nucl. Instr. and Meth. A 611 (2009) 25 [arXiv:0907.3577 [physics.ins-det]].
- [3] R. Wigmans, “The DREAM project: Results and plans,” Nucl. Instr. and Meth. A 572 (2007) 215.
- [4] N. Akchurin *et al.*, “Beam test results from a fine-sampling quartz fiber calorimeter for electron, photon and hadron detection”, Nucl. Instr. and Meth. A 399 (1997) 202.
- [5] Akchurin N. *et al.*, Nucl. Instr. and Meth. A 533 (2004) 305.
- [6] Akchurin N. *et al.*, Nucl. Instr. and Meth. A 536 (2005) 29; A 537 (2005) 537; A 548 (2005) 336; A 550 (2005) 185.
- [7] G. Gaudio, for the DREAM collaboration, “New Results from the DREAM project” proceedings of the VCI2010 conference, Vienna (2010).
- [8] J.C. Brient and H. Videau, “The calorimetry at the future e+e- linear collider”, (2002) [arXiv:hep-ex/0202004].
- [9] The CALICE collaboration web-page: <https://twiki.cern.ch/twiki/bin/view/CALICE/>.
- [10] The CALICE collaboration, “Construction and commissioning of the CALICE Analog Hadron Calorimeter Prototype”, arXiv:1003.2662 [physics.ins-det], submitted to JINST.
- [11] F. Simon, C. Soldner, “Uniformity Studies of Scintillator Tiles directly coupled to SiPMs for Imaging Calorimetry”, arXiv:1001.4665v1 [physics.ins-det], submitted to Nucl. Instr. and Meth. A.
- [12] K. Kotera, for the CALICE collaboration, “Study of the Granular Electromagnetic Calorimeter with PPDs and Scintillator Strips for ILC”, proceedings of the VCI2010 conference, Vienna (2010).
- [13] K. Seidel, for the CALICE collaboration, “Particle Showers in a Highly Granular Hadron Calorimeter” proceedings of the VCI2010 conference, Vienna (2010).
- [14] F. Simon for the CALICE Collaboration, “Energy Reconstruction of Hadron Showers in the CALICE Calorimeters”, arXiv:0911.4575 [physics.ins-det].
- [15] G. Drake *et al.*, “Resistive Plate Chambers for hadron calorimetry: Tests with analog readout”, Nucl. Instr. and Meth. A 578 (2007) 88.
- [16] Q. Zhang *et al.*, “Environmental dependence of the performance of resistive plate chambers”, JINST 5 P02007 (2010).
- [17] R. Kieffer, for the CALICE collaboration, “Development of a Semi-Digital Hadronic Calorimeter Using GRPCs for Future Linear Collider Experiments” proceedings of the VCI2010 conference, Vienna (2010).
- [18] J. Yu *et al.*, “Development of GEM Based Digital Hadron Calorimeter”, submitted to IEEE NSS09. 2009. Orlando, FL, USA.
- [19] A. White *et al.*, “Development of GEM-based Digital Hadron Calorimetry using the SLAC KPcX Chip”, submitted to proceedings of the Micro-Pattern Gas Detector Workshop, Crete (2009).
- [20] C. Adloff *et al.*, “MICROMEGAS chambers for hadronic calorimetry at a future linear collider”, JINST 4 P11023 (2009).
- [21] C. Adloff *et al.*, “Beam test of a small MICROMEGAS DHCAL prototype”, JINST 5 P01013 (2010).
- [22] J. Hoff *et al.*, “A custom integrated circuit for calorimetry at the International Linear Collider”, IEEE Nucl. Sci. Symp., Puerto Rico, 2005, FERMILAB-CONF-05-509.
- [23] B. Bilki *et al.*, arXiv:0802.3398 [physics.ins-det]. 2008 JINST 3 P05001. B. Bilki *et al.*, arXiv:0902.1699 [physics.ins-det]. 2009 JINST 4 P04006. B. Bilki *et al.*, arXiv:0901.4371 [physics.ins-det]. 2009 JINST 4 P06003. B. Bilki *et al.*, arXiv:0908.4236 [physics.ins-det]. 2009 JINST 4 P10008.
- [24] The CALICE collaboration, “CALICE Report to the Calorimeter R&D Review Panel”, arXiv:1003.1394v1 [physics.ins-det], (2010).
- [25] J. Repond *et al.*, “Design and Electronics Commissioning of the Physics Prototype of a Si-W Electromagnetic Calorimeter for the International Linear Collider”, JINST 3 P08001 (2008).
- [26] D. Jeans, for the CALICE collaboration, “CALICE Silicon-Tungsten ECAL”, proceedings of the VCI2010 conference, Vienna (2010).
- [27] The SPIDER collaboration web-page: <https://heplnm061.pp.rl.ac.uk/display/spider/Home>.
- [28] SPiDeR Collaboration, N.K. Watson *et al.*, “DESY PRC Report”, Oct. 2009.
- [29] The International Large Detector (ILD) Letter of Intent, <http://www.ilcild.org/documents/ild-letter-of-intent/LOI.pdf>.
- [30] <http://asic.austriamicrosystems.com/>.
- [31] G. Bondarenko, P. Buzhan, B. Dolgoshein, V. Golovin, E. Guschin, A. Ilyin, V. Kaplin, A. Karakash, R. Klanner, V. Pokachalov, E. Popova, K. Smirnov, Nucl. Instr. and Meth. A 442 (2000) 187.
- [32] P. Buzhan, B. Dolgoshein, L. Filatov, A. Ilyin, V. Kantzerov, V. Kaplin, A. Karakash, F. Kayumov, S. Klemm, E. Popova, S. Smirnov, Nucl. Instr. and Meth. A 504 (2003) 48.
- [33] Z. Sadygov *et al.*, “Microchannel avalanche photodiode with wide linearity range”, arXiv:1001.3050 [physics.ins-det].
- [34] M.V. Danilov, “Particle Detector R&D”, Review Talk at the Lepton and Photon Symposium, Uppsala, 2005, arXiv:physics/0512004v1 [physics.ins-det].
- [35] A. G. Stewart, L. Wall, J. C. Jackson, “Properties of silicon photon counting detectors and silicon photomultipliers”, Journal of Modern Optics, 1362-3044, Volume 56, Issue 2, First published 2009, Pages 240-252.
- [36] A. N. Ottea, B. Dolgoshein, H. G. Moser, R. Mirzoyana, M. Teshimaa, “Status of Silicon Photomultiplier Developments as optical Sensors for MAGIC/EUSO-like Detectors”, 29th International Cosmic Ray Conference, Pune (2005) 00, 101-106.
- [37] P. Eckert, W. Shen, H.-C. Schultz-Coulon, R. Stamen, “Characterisation Studies of Silicon Photomultipliers for a Calorimeter for the ILC”, Workshop on New Photon-Detectors (PD09), Matsumoto, Japan, 2009, submitted to Nucl. Instr. and Meth. A.
- [38] N. Anfimov, “Novel Micropixel Avalanche Photodiodes (MAPD) with super high pixel density”, proceedings of the VCI2010 conference, Vienna (2010).
- [39] J. Ninkovic, “The First measurements on SiPMs with Bulk Integrated Quench Resistors”, proceedings of the VCI2010 conference, Vienna (2010).
- [40] Auffray, E.; Abler, D.; Lecoq, P.; Dujardin, C.; Fourmigue, J.M.; Perrodin, “Dual readout calorimeter with heavy scintillating crystal fibers”, IEEE Nuclear Science Symposium Records, N55-6, 2008.